Labeling the lines: A test of a six-mechanism model of chromatic detection

Timothy G. Shepard College of Optometry, The Ohio State University, Columbus, OH, USA

Safiya I. Lahlaf Department of Psychology, Northeastern University, Boston, MA, USA

Rhea T. Eskew, Jr. Department of Psychology, Northeastern University, Boston, MA, USA

Six linear chromatic mechanisms are sufficient to account for the pattern of threshold elevations produced by chromatic noise masking in the (L,M) plane of cone space (Shepard, Swanson, McCarthy, & Eskew, 2016). Here, we report results of asymmetric color matching of the threshold-level tests from that detection study and use those matches to test the detection model. We assume the mechanisms are univariant labeled lines (Rushton, 1972; Watson & Robson, 1981), implying that the chromaticities of physically different stimuli that are detected by a single mechanism should all be the same—they are postreceptoral metamers—but the chromaticities of two stimuli detected by different mechanisms should be different. The results show that color matches fall into six clusters in CIE (u′,v′) space (across all the noise conditions) and that these clusters correspond closely to the six mechanisms in the model. Most importantly, where the detection model determines that a given test angle is detected by different mechanisms under different noise conditions, the hue of that test angle changes in a consistent way. These color matches allow us to apply a color label to each of the mechanisms, confirm the six-mechanism model, and quantify the hue signaled by each mechanism.

Introduction

The cardinal model of color mechanisms (Krauskopf, Williams, & Heeley, 1982; Lennie & D'Zmura, 1988) consists of three bipolar linear combinations of signals from the cones: ±[L − M], ±[S − (L + M)], ±[L + M], or, treating each polarity separately, six rectified mechanisms. This model has been shown to be incorrect, in part because it predicts that the effects of chromatic masking or habituation are broadly rather than narrowly tuned in color space, while in fact, noise masking or habituation can produce narrowly tuned (selective) effects (see reviews by Eskew, 2009; Hansen & Gegenfurtner, 2013; Krauskopf, 1999).

Recently we (Shepard et al., 2016) measured forced-choice detection thresholds for stimuli that only modulated the L and M cones, under four different chromatic noise conditions. Two of the noise chromatic angles were near the ends of the no-noise detection contour. Hansen and Gegenfurtner (2006, 2013) showed that noise vectors that intersect the detection contour near the contour's ends, and therefore have color directions that are approximately parallel to the long flanks of the contour, cause the contour to be become elongated, roughly in the same chromatic direction as the noise, an effect that the cardinal model does not capture. We replicated the selective masking that Hansen and Gegenfurtner (2013) reported. However, our chromatic detection model accounts for selective masking even though it contains only six (rectified) mechanisms, not the large number of mechanisms used by Hansen and Gegenfurtner (2006) in computing their model predictions (see appendix to Shepard et al., 2016). In the current study, we quantify the hues produced by the mechanisms in our model using asymmetric color matching.

A schematic of our model is shown in Figure 1. In Shepard et al. (2016), the mechanisms were labeled with single-letter mnemonics for the hues they signal: (R)ed, (G)reen, (Y)ellow, (B)lue, (O)range, and (P)urple. Those hues were determined approximately and informally using the observers' verbal report of the predominant hues of the threshold tests measured in that study. The top and middle pairs of mechanisms in

Citation: Shepard, T. G., Lahlaf, S. I., & Eskew, R. T., Jr. (2017). Labeling the lines: A test of a six-mechanism model of chromatic detection. *Journal of Vision*, *17*(13):9, 1–18, doi:10.1167/17.13.9.

doi: 10.1167/17.13.9 Received November 6, 2016; published November 8, 2017 ISSN 1534-7362

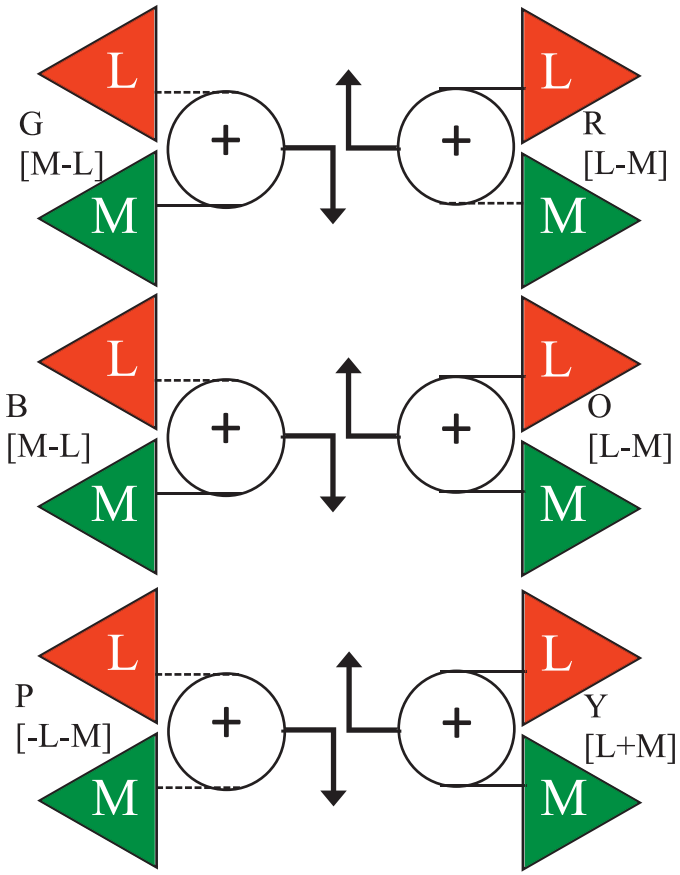

Figure 1. Six-mechanism model (modified from Shepard et al., 2016). The dashed lines represent sign-inverted (negative) cone inputs. Each mechanism is half-wave rectified, as suggested by the output arrow pointing in only one direction. The cone contrast weights for this model are given in Table A1. Four of these mechanisms (R & G and B & O) are "quasi-paired," having nearly equal and opposite L and M cone weights. Two mechanisms (Y and P) have additive L and M cone inputs and are asymmetric (unpaired). Although B & G and R & O, have the same *signs* of L and M cone inputs, they differ by having different relative L and M cone weights.

Figure 1 (R & G and O & B) take the weighted differences of the L and M cone signals, with different weights for all four mechanisms (within each row, the weights are of opposite signs and similar but not identical magnitudes, so we refer to them as "quasi-paired"). The bottom pair of mechanisms (Y and P) takes the sum of the L and M cone signals, again with weights that are of opposite signs for the two mechanisms in the row. Table A1 gives the cone contrast weights (based on table 1 of Shepard et al., 2016). We have not yet determined which of these mechanisms get inputs from the S cones, but presumably at least Y and P do.

The model of Shepard et al. (2016) differs in one important way from the cardinal model: four of our six detection mechanisms have opposed L and M cone inputs (R, G, O, and B, with different relative weights), rather than just two, as in the cardinal model (L-M and M-L). This is the critical feature that allows the model to account for selective masking in the (L,M) plane. Noise angles that are approximately parallel to the long flanks of the contours can cause different combinations of R, G, O, and B to become most sensitive and thus determine threshold, tilting the overall detection contour, as observed by Hansen and Gegenfurtner (2013); see also Shepard et al. (2016, figure 9). Other models that have been proposed to account for selective masking generally contain many more "higher-order" mechanisms (e.g., Hansen & Gegenfurtner, 2006; Li & Lennie, 1997) than the six in our model.

Our model has not yet been tested in full LMS color space, and it is possible that additional color mechanisms may have to be added to account for other data, which would make our model have more mechanisms than the cardinal model. However, in the (L,M) plane, the six-mechanism model provides an excellent and parsimonious account of detection across a variety of masking noise conditions (Shepard et al., 2016).

The main purpose of the present color matching study was to determine the hue of the test stimuli that we had used in the detection experiment and relate the hues to the mechanisms in Figure 1, using the following properties of mechanisms. We define a mechanism as a "fixed (relative) combination of cone signals that is correlated with the observer's behavior in psychophysical experiments" (Eskew, 2008, p. 103). Mechanisms are assumed to be univariant, which implies that when two stimuli are detected by one and only one mechanism, there is some relative intensity at which the two stimuli cannot be discriminated from one another. In addition, they are "labeled lines," which implies that when two stimuli are detected by different mechanisms, they must be discriminable from one another at all relative intensities (Krauskopf et al., 1986; Mullen & Kulikowski, 1990; Watson & Robson, 1981). Taken together, these assumptions imply that each mechanism is characterized by one and only one hue, and the minimum number of color match clusters made to threshold-level stimuli is the number of mechanisms in the detection model. If, for example, the detection model has 16 mechanisms, then there should be at least 16 clusters of color matches. Further discussion of how the number of clusters is related to the number of mechanisms is provided in the Mechanism hues section in Results and discussion.

In our detection model (Figure 1), thresholds mediated by a single mechanism follow an energy versus noise (EvN) relationship based upon the theory of noise masking (Giulianini & Eskew, 2007; Wang,

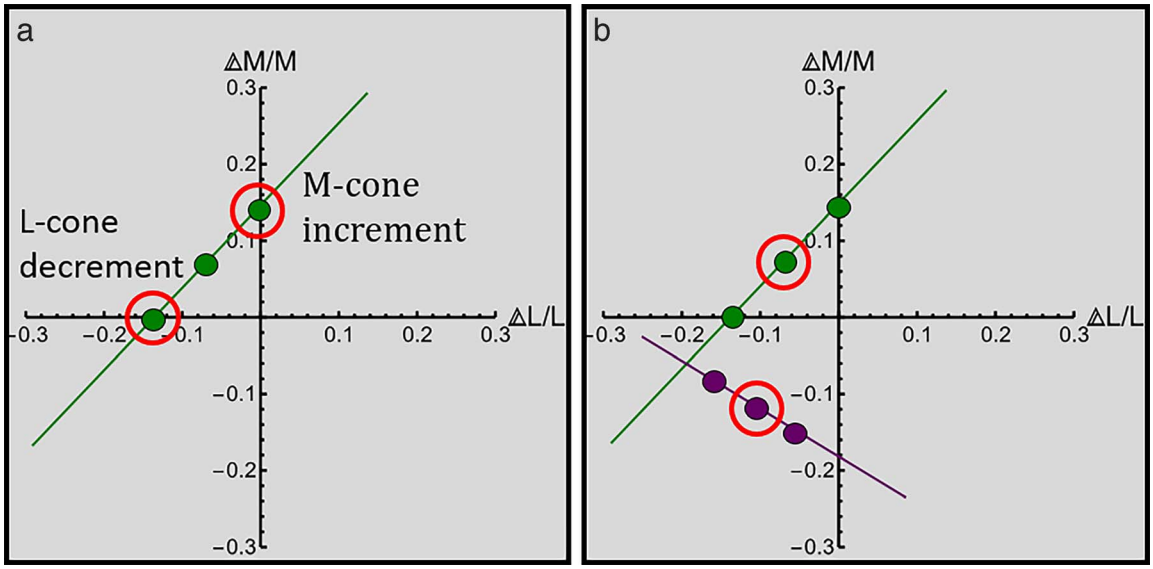

Figure 2. The lines represent threshold responses of one (a) or two (b) hypothetical detection mechanisms in the (ΔL/L, ΔM/M) plane, with the colored disks representing schematic data. The position of each disks gives the threshold coordinates and the color of the disks represents the match to the color appearance of the test. The interpretation of the color matches is based on two properties of a mechanism: (a) Univariance implies that physically different threshold tests that are detected by a single mechanism should produce metameric color matches. For example, examine the two disks in red circles: an M-cone increment test (greenish) may produce the same color match as a L-cone decrement test (greenish) because both test thresholds are detected by the same univariant mechanism. (b) Labeled lines imply that when tests lie on two different mechanism lines as do the two-circled disks, they should be matched with two different hues. A 225° (purplish) test should produce a different color match than the 135° (greenish) test since they are detected by two separate mechanisms.

Richters, & Eskew, 2014), in which the threshold contrast energy of the test is linearly related to the noise contrast power (both quantities being proportional to the squared contrast). Each mechanism has the same mechanism color angle (because it has the same relative cone weights) across all noise conditions (for details, see Shepard et al., 2016, table 1 and appendix), as a result of which each mechanism threshold line has the same slope under all noise conditions. This is because the threshold line is perpendicular to the vector of weights, the mechanism vector (Eskew, McLellan, & Giulianini, 1999). Moreover, the threshold elevation produced by chromatic noise at a given angle is proportional to the squared cosine of the difference between the mechanism and noise color angles, meaning that the distance from the origin to the mechanism threshold line is determined by theory rather than fit freely to data. This means that the model can and does place some mechanism threshold lines outside of the set of observed thresholds in a particular noise condition, because the model asserts that those mechanisms do not contribute to threshold in that condition; the tuning and sensitivity of the mechanism is known from measuring thresholds across multiple noise conditions. These model features are derived from theory and highly constrain the fit of the detection model to the data.

In the present study, the observers from Shepard et al. (2016) were presented with their own threshold level stimuli, as measured in the previous study. They matched their own threshold stimuli in color using a suprathreshold matching spot, an asymmetric color matching procedure (Wyszecki & Stiles, 1982, chapter 5). The labeled-line and univariance properties enable a theoretical interpretation of the color matches. Hypothetical examples are shown in Figure 2. An M-cone increment test may produce the same color as a L-cone decrement test because both test thresholds lie on the same univariant mechanism threshold line (Figure 2a). All other color matches along this mechanism line should also be of the same chromaticity—they are postreceptoral metamers. The labeled line assumption implies that when tests lie on two different mechanism lines, they should be matched with two discriminably different chromaticities. In the example of Figure 2b, a 135° threshold test should produce a different color match from a 225° test, since they are detected by two separate mechanisms.

It is important to keep in mind that the detection model was determined solely by the two-alternative (2AFC) threshold data in Shepard et al. (2016); it was fit to those data in the earlier paper, prior to measuring the color matches reported here. By comparing the

color matches with the mechanism threshold lines, we can "label the lines" and test the model.

Methods

Observers

The same three well-practiced observers who participated in the detection experiment (Shepard et al., 2016) also participated in the color matching experiment presented here. These observers were not completely naïve; all knew that the model contained six detection mechanisms, and the color names associated with the six mechanisms (see Non-naïve observers in the General discussion section). TGS is male, myopic (correction of −3.2D), and was age 35 at the start of this experiment. CLM is female, myopic (−1.0D), and was age 19. SAF is female, emmetropic, and was age 19. All had normal scores on the Farnsworth-Munsell 100 Hue Test (Farnsworth, 1943) and the Ishihara Plates. Observers gave informed consent. Northeastern University's Institutional Review Board approved the research protocol; the procedures comply with the Declaration of Helsinki.

Apparatus

Test and noise stimuli were created on a Power Macintosh computer and displayed on a Sony GDM-F520 CRT monitor running at 75 Hz using an ATI Radeon 7500 video board (ATI Technologies Inc., Markham, ON, Canada) with a driver verified to support the 10-bit digital-to-analog converters (DACs). Calibrations were performed with a Photo Research PR-650 spectroradiometer (Photo Research Inc., Syracuse, NY). Spectroradiometric calibration of the experimental display was performed at 4 nm intervals across the spectrum and this monitor was linearized with gamma correction lookup tables. The color matches were determined on a 15-inch MacBook Pro, using an Intel HD 4000 graphics card, that was placed at right angles to the experimental monitor; a piece of black cardboard was used to mask the screen, showing only the hue-saturation-value wheel used for the matches (see Procedure section), which subtended 8°. This matching display was not gamma corrected; instead of the chromaticity of the match being calculated from software-supplied values, the chromaticity of each match was measured as in the Procedure section.

All experiments were conducted in a dark room. Head position was stabilized with a chin and forehead rest. Viewing distances were 71 cm to the experimental display, and 40 cm to the matching display.

Observers were corrected to normal visual acuity using the appropriate standard ophthalmic trial lens, which was placed in front of their dominant eye; the other eye was patched. The trial lens was used to view the experimental monitor but was not used when the observer made the color matches on the matching display. Neither of the myopic observers reported any difficulty when selecting a color match on the matching display without refractive correction.

Test and noise stimuli

Cone isolating stimuli and their mixtures were created using standard methods (Estevez & Spekreijse, 1982). The stimuli are identical to those used by Shepard et al. (2016): Gaussian blobs ($\sigma = 1°$, 333 ms sawtooth time course). Their chromaticities are specified by their polar angles in the ($\Delta L/L$, $\Delta M/M$) plane of cone contrast space (Brainard, 1996), with 0° and 90° representing the L and M cone increment directions, respectively. The bipolar noise has two complementary angles, separated by 180°, and the noise direction will be identified by the angle of the first pole (e.g., the noise direction 42°/222° will simply be called 42° noise). S cones were not modulated by any of the test or noise stimuli.

The backgrounds of the test and color matching displays were the same mid-gray (CIE $x = 0.30$, $y = 0.31$). The tests were circular Gaussian blobs ($\sigma = 1°$), presented with a waveform that abruptly shifted to the desired contrast and then ramped linearly to zero over 333 ms. A total of 248 threshold-level tests (all of the thresholds measured in Shepard et al., 2016) were used as the stimuli for the current color matching study (92 for observer TGS, 94 for CLM, and 62 for SAF).

The masking noise consisted of two-pixel horizontal lines, each subtending 0.05° in height, with the test appearing in the 0.05° regions between noise lines (i.e., noise and test lines were half-toned). The noise lines covered a 10° × 10° region of the screen, centered on the test. As discussed in Shepard et al. (2016), the noise color directions were selected to lie near the corners of the detection contour, where the underlying mechanisms are of equal sensitivity so their mechanism threshold lines intersect; these are the noise directions where Hansen and Gegenfurtner (2013) found selective masking effects (see Introduction). The noise contrast was always 90% of the maximum available at the noise direction; in cone contrast units, the noise cone contrast vector length $|\mathbf{n}|$ was 0.498, 0.414, and 0.267 for the 42°, 48°, and 64° noises, respectively. In the no-noise condition, the noise lines were drawn with the noise contrast set to zero. Further

details of the test and noise stimuli may be found in Shepard et al. (2016).

Procedure

Each observer was presented with his or her own threshold-level tests under the same noise conditions that had been used to measure the thresholds: one no-noise and up to three with noise (noise angles of 42°, 48°, and 64° in the ΔL/L, ΔM/M plane of cone contrast space). Author TGS and observer CLM participated in all four noise conditions. Author SAF participated in three noise conditions, since SAF only collected thresholds in these three conditions in the detection experiment (Shepard et al., 2016).

For color matching, test angles were blocked by noise condition and run in random order within that block; the observer did not know which test was being presented. The observer was shown the test on the experimental display, fixed at its measured threshold from the detection experiment (Shepard et al., 2016), in one of two temporal intervals, just as in the threshold measurement procedure, in the presence of the noise (except in the no-noise condition). Intervals were demarcated by tones.

Observers were given auditory feedback regarding their choice of the interval containing the test. Only if the observer correctly selected the test interval was he or she permitted to make a color match (described next). The purpose of this procedure was to confirm that the observer's thresholds (from Shepard et al., 2016), which were originally measured up to several months earlier, had not changed substantially and that the observer was making a match to a test flash they had actually just seen, rather than basing the match upon memory of recently-viewed flashes.

On presentations in which the correct interval was selected, the observer then turned to the matching display positioned off to the side and selected a matching chromaticity on a hue-saturation-value (HSV) color wheel (Figure 3, left). When satisfied with the match on the HSV wheel, the observer was presented with a disk of that same matching chromaticity on the matching display, which was approximately the same visual angle as the Gaussian test (Figure 3, right). This disk was presented on the laptop against a gray background that matched the luminance and chromaticity of the main experimental monitor's background. If the match was confirmed, the final HSV values of the match were recorded and a new test angle was selected. Five matches were made at each test angle, chosen in random order, in each noise condition; matches in a given noise condition were collected in at least two sessions on different days. The observer was allowed up to 50 trials to confirm a match for each test angle. If a match was not confirmed after 50 trials, then that test angle was to be retested later on in the session (but none of the observers used all of the 50 allotted trials). After the match to a given test angle was completed, the experimenter confirmed that the threshold contrast used was correct by verifying that the observer had correctly selected the test interval in about 80% of the presentations.

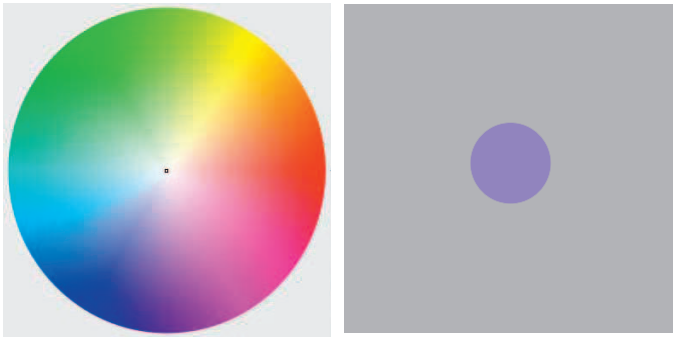

Figure 3. HSV color wheel (left) from Microsoft PowerPoint, used to make the initial match. Confirmatory match (right) was a colored disk of approximately the same size as the test stimulus, displayed on a gray background that had the same chromaticity and approximately the same luminance as the experimental monitor.

Although observers were free to vary the brightness of the matching stimulus, none of them did, so the analysis here is based only upon hue and saturation. After the experiment was completed, the CIE 1931 (x, y, Y) chromaticity coordinates of each of the five matching disks were measured on the matching display with an X-Rite i1Display Pro colorimeter (X-Rite, Grand Rapids, MI). These five chromaticities were averaged; the centroid of the five matches was then transformed to CIE (u′,v′) space. The averaged match coordinates of each test were used in all further analysis of the color matches, and are plotted in the data figures as black dots.

Results and discussion

The first step in the analysis was to pool all the (u′,v′) values for a given observer (combining all the matches across noise conditions) and subject the entire set of matches to a single-linkage cluster analysis (using Mathematica's FindClusters routine), which does not require constraining the number of clusters. This analysis parallels the modeling in (Shepard et al., 2016), in which the detection model was fit to the data from all noise conditions simultaneously (however, the color matching experiment was conducted after the detection

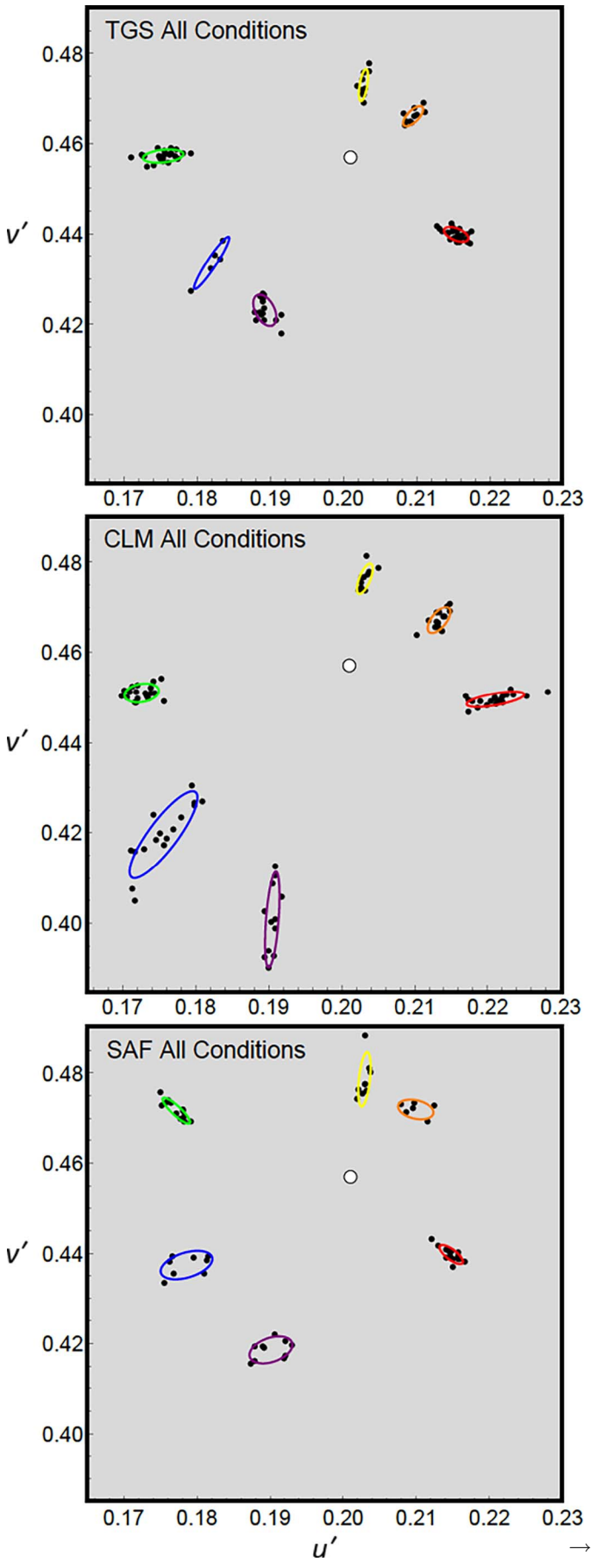

model had been fit to the threshold data). For each observer, six clusters of color matches were found by the cluster analysis. However, given that the clusters were completely nonoverlapping, the cluster analysis is actually unnecessary.

For each cluster considered separately, a 95% confidence ellipse around the centroid was computed based upon principal components analysis. These ellipses are colored to approximately represent the hue of the stimuli in the cluster. Figure 4 shows all of the color matches, along with the six ellipses, from the pooled analysis for each of the three observers. Each observer's six ellipses will also be shown in the left hand panels of Figures 5–8.

Figures 5–8 (right panels) show the thresholds and model from the detection experiment (Shepard et al., 2016) and the color matches from the current color matching study (left panels). Before describing the results in each of the four noise conditions, we here provide a preview of the elements that are shown in the pairs of panels of all of these figures. The right-hand panels represent the (ΔL/L, ΔM/M) plane of cone contrast space, with the origin representing the gray background adapting field and the axes representing the modulation of the cones relative to the quantal catch produced by the mean adapting field. Four things are shown on the cone contrast plots. (a) The (ΔL/L, ΔM/M) coordinates of the disks reproduce the two-alternative forced choice thresholds in the no-noise condition, from (Shepard et al., 2016). These thresholds were the stimuli to which the color matches were made. (b) The colored lines represent mechanism thresholds from the model fit to the detection data by Shepard et al. (2016), and (c) the solid closed contour shows the probability sum of the mechanisms (d). The colors of the disks represent the color matches, and will be discussed below.

The left-hand panels of Figures 5–8 are CIE (u′,v′) diagrams, a projective transformation of cone contrast space. Each plot represents seven things: (a) The small black dots represent color matches in that particular noise condition (subsets of the dots in Figure 4); (b) The colored ellipses are the confidence regions based on the pooled matches as shown in Figure 4; (c) The range of angles in brackets comprise the cone contrast test angles which generated the matches in the nearby ellipse; (d) The colored disks are the cone contrast

←

Figure 4. Each black dot represents the mean of five color matches (one mean per test angle per noise condition), from all noise conditions combined, along with the measured white point (white disk) of both of the experimental and matching monitors, plotted in (u′,v′) coordinates. Panels a, b, and c represent observers TGS, CLM, and SAF, respectively.

thresholds shown in the right-hand panel, transformed to (u′,v′) space; (e) The colored lines are the (u′,v′) representation of the mechanism thresholds shown in the right-hand panel and (f) the closed contour is the transformation of their probability sum; and (g) The white disk represents the measured white point on both the experimental and matching monitors (corresponding to the origin of the cone contrast diagram).

No-noise condition

First we describe the color matches from the no-noise condition, beginning with Figure 5e, at bottom left, for observer SAF. There are five dots within or near the green confidence ellipse, representing the mean matches of the five test stimuli in the no-noise condition that fall into this cluster; these test stimuli have cone contrast angles ranging from 64° to 195° (the values in square brackets near the ellipse). Four tests (cone contrast angles ranging from 42° to 52°) fall into the yellow cluster, two into orange, four into red, four into purple, and only one in the blue cluster. There is one match in each of the red, yellow, and green clusters that is hidden by another match with very similar coordinates.

Panels 5a and 5c show the mean no-noise color matches as black dots for the other two observers, with the same conventions used for SAF in panel 5e. Note that for both of these observers, unlike SAF, no matches fall into the orange or blue clusters; recall that the clusters are based upon pooling the data across noise conditions as plotted in Figure 4, and (as shown below) orange and blue matches were made by TGS and CLM to tests in the presence of noises, but not in the no-noise condition.

The coordinates of the colored disks in both the left- and right-hand panels represent the detection thresholds from Shepard et al. (2016). To make the (u′, v′) plots legible, the thresholds were increased by a factor of 5 (and the mechanisms were similarly *decreased* in sensitivity by a factor of 5) in the no-noise condition before the transformation from cone contrast to (u′,v′). The positions of these disks in the left-hand panel confirm that the (u′,v′) coordinates of the threshold stimuli themselves do *not* fall into six clusters, but are distributed around the white point (white circle). The clustering only occurs in the matches to the threshold stimuli (black dots in the left panels), not in the threshold stimuli to which the matches are made (colored disks in left and right panels). Thus, the clustering is not produced by the transformation from cone contrast space to (u′,v′) space, nor are the observers simply reproducing the chromaticities of the tests in this asymmetric matching procedure. The clustering represents postreceptoral metamerism, in which physically different test stimuli produce the same match.

In the (u′,v′) plots, the cone increment and decrement thresholds, as well as the 45° and 225° thresholds in cone contrast space (the thresholds at the ends of the cone contrast detection contours), are denoted by text labels. Note that the L+ and M− thresholds, and the L− and M+ ones, have similar chromaticities in this condition; in this projective transformation of cone contrast space they are so similar for observers CLM and SAF that the L+ and M+ points are obscured by the M− and L− ones, respectively.

For each test angle, the detection threshold points have been colored to approximately represent the mean hue of the five color matches that the observer made for that test angle, with the saturation increased to make the color visible in the figure; the precise chromaticities are represented by the black dots in the left-hand panel. Because these hues represent actual observations, the hue of the symbol differs slightly for nearby test angles for a given observer. Similarly, because observers differ somewhat in their color matching, there are differences between observers for the same test angle. For example, the M cone decrement tests were matched with a slightly more reddish-blue stimulus by observer SAF (disk at 270° in panel f) compared to CLM (disk at 270° in panel d), as can also be seen in the dots in the (u′,v′) plots, where SAF's reddish cluster has somewhat lower v′ values than CLM's. The color matches show several such quantitative individual differences, as do the detection model fits in Shepard et al. (2016), but qualitatively, the matches are similar for all observers.

The colored lines represent the *mechanism* thresholds, from the model of Shepard et al. (2016). The mechanism threshold lines in both cone contrast and (u′,v′) spaces have been colored with a hue that represents the approximate color category of the matches to the thresholds that fall along, or very near, the lines, with the same six colors used for all observers. Some of these threshold lines have been dashed to make them more distinguishable from other figure elements. Four of the mechanism threshold lines (R, G, O, and B) have positive slopes and form the flanks of the detection contour in cone contrast space (right panels), and two (Y and P) have negative slopes and cover the ends of the detection contour. In (u′,v′) spaces (left panels), the Y and P mechanism thresholds are roughly horizontal, with Y on top of and P below the white point. R and G are on the right and left of the white point, and O and B are (roughly) to the upper right and lower left, respectively, in (u′,v′).

Note that for TGS and CLM, the detection model places the O and B mechanism lines clearly outside of

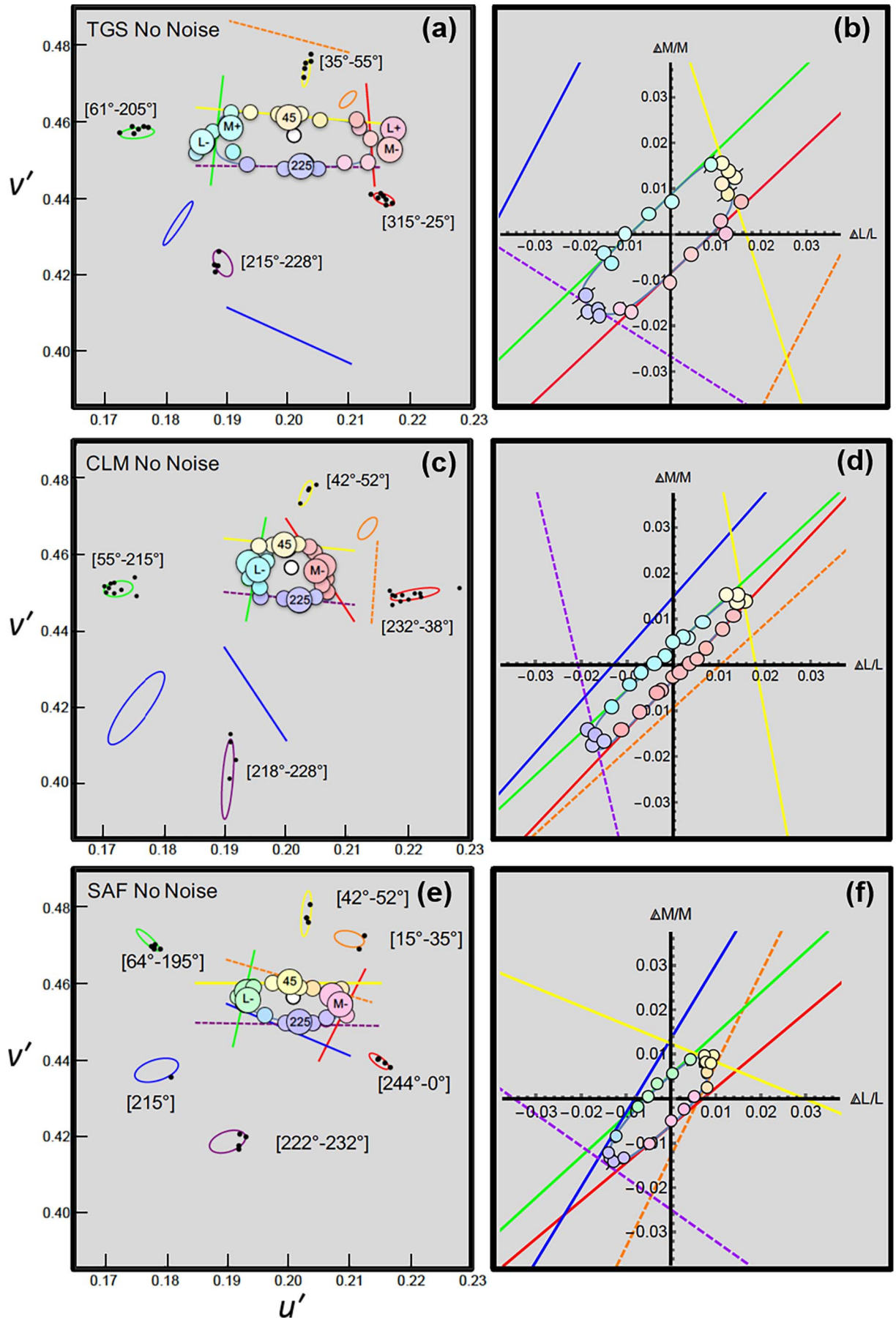

→

←

Figure 5. No-noise condition. The three rows represent observers TGS, CLM, and SAF. Right panels: cone contrast diagram. The origin represents the background of the experimental monitor, and the axes show the relative modulations of the L and M cones. The (ΔL/L, ΔM/M) coordinates of the disks reproduce the two-alternative forced choice thresholds in the no-noise condition from Shepard et al. (2016). The colored lines are the model mechanism thresholds. The colors of each disk represent the mean color match made to the stimulus at those coordinates. Left panels: (u′,v′) chromaticity diagram. The white disk is the measured chromaticity of both the experimental and matching monitor (corresponding to the origin of the right-hand panels). The black dots give the chromaticities of the mean color matches for each test in the no-noise condition. The colored ellipses are reproduced from Figure 4. The numbers in square brackets next to the clusters represent the range of cone contrast test angles producing color matches in that cluster. The colored disks are the projection, into (u′,v′) space, of the cone contrast coordinates of the thresholds on the right, with the same coloring. Key cone contrast test angles are denoted by labels on the disks. See text for details.

the thresholds, as shown in both color spaces. Thus, according to the detection model, these mechanisms do not contribute to detection in this condition, and the slope and placement of the mechanism lines depend only upon thresholds measured in the other noise conditions (see Introduction and Shepard et al. [2016] for discussion). The lack of contribution of these mechanisms to detection exactly parallels the lack of blue and orange color matches—there are no dots in the blue and orange ellipses—independently determined.

For all observers, the number of clusters of color matches and the number of mechanisms detecting the tests agrees perfectly, despite these two types of data being collected independently (and weeks or even months apart). Test stimuli within any given cluster are generally aligned with only one mechanism line in the model fit (univariance), and each mechanism line is characterized by a different cluster (labeled lines).

42° noise

Figure 6 shows data from the 42° noise condition, in the same format as Figure 5. The overall detection contour in cone contrast space is elongated and tilted in the direction of the noise (right-hand panels); this tilt is slight in the cone contrast space used here, but would be larger if plotted in a threshold-normalized cone excitation space, as shown by Hansen and Gegenfurtner (2013) and Shepard et al. (2016). The (u′,v′) plots also represent the noise effect as large: the no-noise contours in Figure 5 (left) are roughly horizontal, while in the 42° noise condition the (u′,v′) contours are roughly vertical (recall that the no-noise thresholds in Figure 5 were increased by a factor of 5 in the (u′,v′) plots; no rescaling was used in any of the other conditions).

The theoretical constraints of the model require the mechanisms to have the same relative cone weights, and thus the same mechanism angles, across all of the noise conditions, in cone contrast space or linear transformations of it (see table 1 and the appendix in Shepard et al., 2016 for details). Therefore, the mechanism threshold lines (at 90° to the mechanism angles) have the same slope in cone contrast space (or linear transformations of it) in all of the noise conditions, and their distance from the origin is constrained by the noise power and angle (according to the quantitative model developed in Shepard et al., 2016, and Wang et al., 2014). However, because (u′,v′) is a *projective* transformation of cone contrast space, the mechanism lines do not in general have the same slopes across noise conditions in (u′,v′). For example, for TGS the R and G lines are nearly vertical in Figure 6a, but tilted slightly inwards in Figure 5a.

Note that Figure 6 shows there is now a set of matches within or near the orange ellipse in CLM's matches (panel c) and that the detection model has the O mechanism now contributing to threshold (panels c and d). The R mechanism lies outside the detection contour for CLM, and correspondingly there are no color matches in the red ellipse. It is important to emphasize that the detection model was fit to the thresholds entirely independently of the color matches (in fact, the detection models were fit months before measuring the color matches). For TGS and SAF, thresholds along the long flanks in cone contrast space are attributed to the R and G mechanisms (panels b and f), whereas for CLM (panel d), the model asserts that the R mechanism has been sufficiently masked so that it does not contribute, and the lower cone contrast flank is attributed to O. The color matches are consistent: TGS and SAF have reddish and greenish matches, whereas the flanks produce orangish and greenish matches for CLM.

In general, the agreement between the two procedures is excellent in this condition, as it is in the no-noise condition. The number of matching clusters again exactly matches the number of detection mechanisms that are sensitive in this condition. However, a discrepancy exists for TGS at the ends of the 42° noise detection contour. According to the detection model, the Y and P mechanisms lie somewhat outside the detection data, and the ends of the contour are served

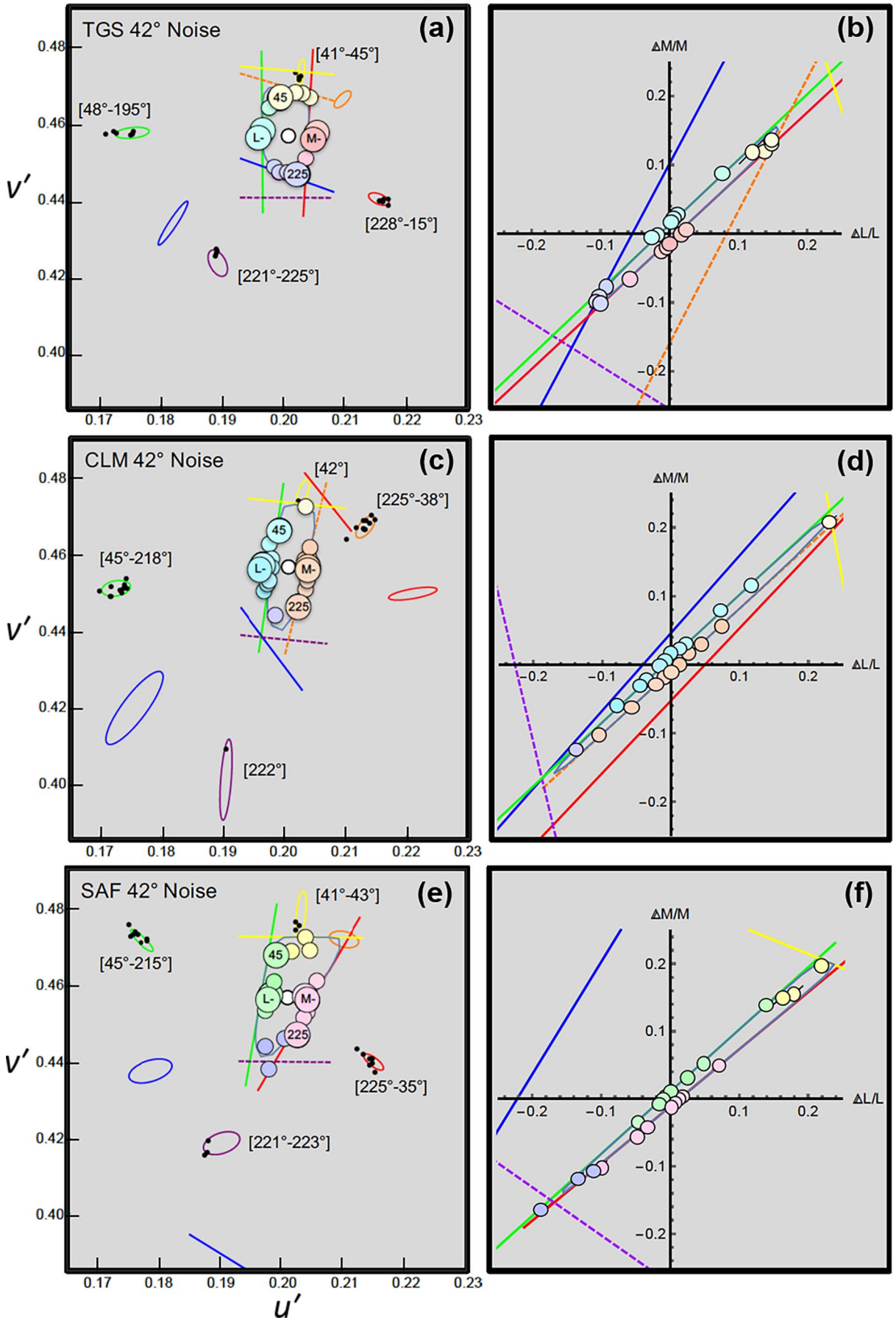

←

Figure 6. 42° noise condition. Format as in Figure 5. Axis scales in the (u′,v′) plots (left panels) are the same as the left panels of Figure 5, but scales in the detection plots (right panels) are expanded to allow for the masking effects of the noise. This noise has masked the O mechanism for SAF to such a degree that it is not visible on the plot.

by the O and B mechanisms. However, the color matches for these thresholds fall into the purple and yellow clusters instead of the blue and orange ones (Figure 6a).[1] This issue will be discussed in the section, Discrepancies involving Y and P in the General discussion.

48° noise

Figure 7 shows the matches, thresholds, and model in the 48° noise condition for CLM and TGS (SAF did not participate in this noise condition). As shown in Figure 7a, TGS's color matching data clusters into five clusters (black dots in the red, green, orange, purple,

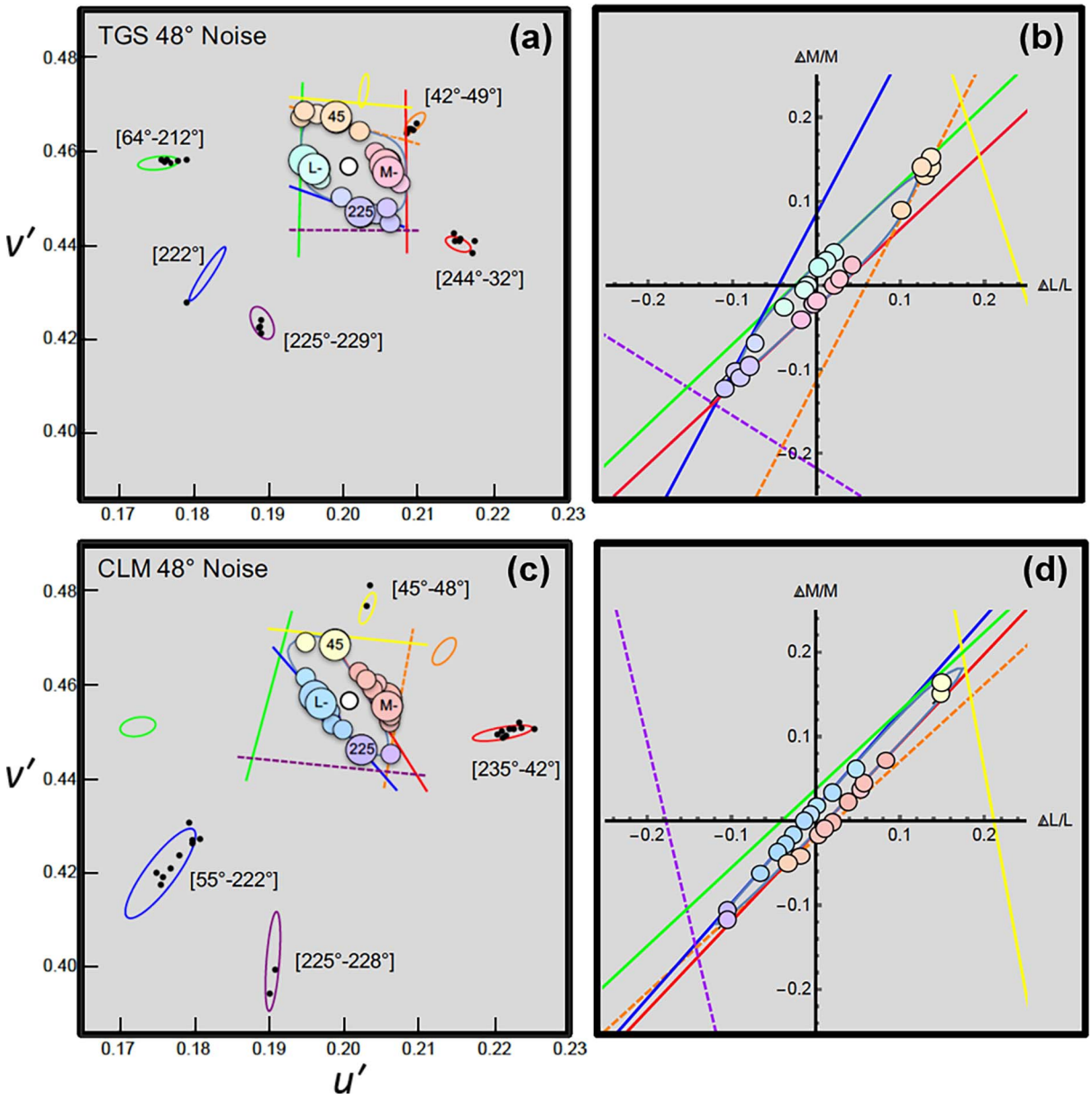

Figure 7. 48° noise condition. Format as in Figure 5. Axis scales in the (u′,v′) plots (left panels) are the same as the left panels of Figure 5, but scales in the detection plots (right panels) are expanded to allow for the masking effects of the noise. SAF did not participate in this noise condition.

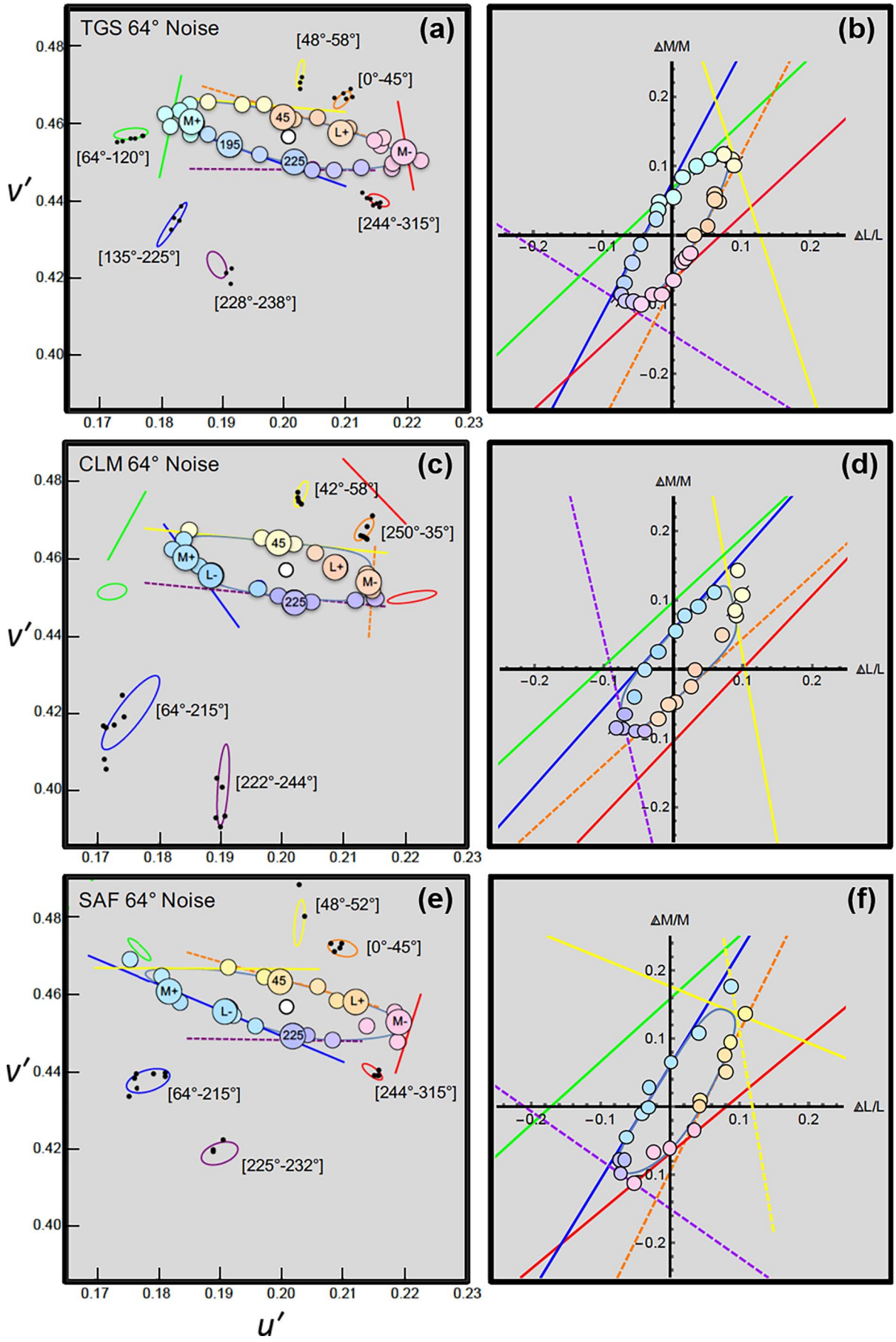

→

←

Figure 8. 64° noise condition. Format as in Figure 5. Axis scales in the (u′,v′) plots (left panels) are the same as the left panels of Figure 5, but scales in the detection plots (right panels) are expanded to allow for the masking effects of the noise. TGS was not tested with the L-cone decrement; instead, the label in his (u′, v′) plot is on the nearby 195° cone contrast stimulus.

and blue ellipses, the last of which has only one match). Similarly, five mechanisms are required to account for TGS's test thresholds (panels a and b). The R and G mechanisms detect the majority of the tests along the long flanks and the O, P, and B mechanisms detect tests near the ends of the contour (i.e., Quadrants I and III in cone contrast space), and the Y mechanism does not contribute to detection in this condition. Therefore, the detection model predicts there will be no color matches falling in the yellow cluster, and this is the case (Figure 7a). It is worth noting that the model slightly overestimates the R and G mechanism thresholds (the data points along the flanks in Figure 7b are consistently slightly inside the red and green lines); the (u′,v′) representation visually exaggerates this extremely small cone contrast difference due to the projective transformation (e.g., reddish disks vs. red line in Figure 7a).

At the upper end of CLM's detection contour in cone contrast space (Quadrant I, Figure 7d), the Y mechanism threshold line lies somewhat beyond the threshold points, but the projection of these points (drawing a line from the origin through the point) intersects the Y line before any other line, so the model predicts that these are Y-detected.

Therefore, CLM's color matches fall into the four clusters (Figure 7c, black dots) that are predicted by the detection model, with the possible exception of the one point near the corner of P and R. Interestingly, the mechanisms that detect the majority of the tests along the cone contrast flanks once again switch with the addition of the 48° noise; according to the detection model, the upper cone contrast flank for CLM is now served by B instead of G, and the lower cone contrast flank by R instead of O (Figure 7d vs. Figure 6d). Note that although O is close to these thresholds in cone contrast units, it is outside the R line—in the projection into (u′,v′) that difference is magnified. This type of switching is what allows the model to account for the approximate alignment of the thresholds with the noise angle, as observed by Hansen and Gegenfurtner (2013). Thus, approximately the same range of test angles that was detected by the R mechanism without noise (Figure 5d) and have matches in the red cluster (Figure 5c) are detected by the O mechanism in the 42° condition (Figure 6d) and have orange matches (Figure 6c); these angles then switch back to red in the 48° noise condition (Figure 7c and d). A given test angle can be detected by different mechanisms in different noise conditions according to the detection model; the mechanism properties (univariance and labeled lines) imply that the color matches should change in a consistent way with the mechanism switching, and they do.

64° noise

Figure 8 shows the matches, thresholds, and model in the presence of the 64° noise. TGS's detection model (colored lines in Figure 8a and 8b) has all six mechanisms contributing to the detection thresholds, and his matches fall into all six clusters (Figure 8a, black dots). CLM's thresholds (colored disks in Figure 8c and 8d) are determined by only four mechanisms, and her color matches fall into the corresponding four clusters (Figure 8c, black dots). Note that the noise has moved the G mechanism out of the way, leaving B to determine threshold; correspondingly, there are no green matches for this observer in this noise condition (compare Figure 8c and d with Figures 5c and d, 6c and d, and 7c and d). SAF's thresholds require five mechanisms (colored lines in Figure 8e and 8f) and the color matches fall into the corresponding five clusters (Figure 8e). The extra (dashed) yellow line in panel f is a possible alternative mechanism threshold locus for the Y mechanism; it is discussed in the Discrepancies involving Y and P section in the General discussion, below.

Note that in the 64° noise condition, the L+ and M− thresholds and the L− and M+ thresholds, have (u′,v′) chromaticities that differ more noticeably than in other conditions. Despite this chromaticity difference, the color matches for L+ and M− are in the orange cluster for CLM (panels c and d), and M+ and L− are matched into the blue cluster by both CLM (panels c and d) and SAF (panels e and f). These are particularly clear examples of postreceptoral metamerism, one in which the pairs of stimuli are not only physically different, but are detected via different photoreceptor types.

In general, the agreement between the two datasets in the presence of 64° noise is again excellent. However, there is one clearly discrepant point for SAF. The 64° test angle (leftmost colored disk in Figure 8e, highest disk in Figure 8f) is matched with a bluish hue, which would be consistent with detection by the B mechanism. However, this point lies beyond the Y mechanism threshold, which implies that this test should be detected by Y and produce a yellow match. This discrepancy, like the one discussed above in connection with Figure 6a and b, involves mechanisms at the ends of the cone contrast detection contour and will be discussed in the section titled Discrepancies involving Y and P.

Noise and color matching

Comparing the color matches across noise conditions—the positions of the black dots in the left panels of Figures 5 through 8—suggests that there is no systematic effect of the noise condition on the matches in a given cluster. Adding noise or altering its chromaticity has no apparent effect on the saturation of the matches (i.e., distance of the black dots to the white point) or their chromaticities within the cluster. The noises raise the contrast required to reach threshold, but, given that the test stimuli are at threshold, the noise has no consistent effect on the color matches. In other words, the subjective strength of the stimulus being matched is the same in each noise condition: there is no effect, contextual or otherwise, of the noise on the matches themselves.

Differential masking

There are a number of instances where the detection model determines that a given test angle is detected by different mechanisms in different noise conditions (due to varying effects of the noises), even though of course a given test angle has the same relative L and M cone excitations, irrespective of noise condition. The agreement between the differential effects of the noise on *thresholds* and on *color matches* shows that the two measurements do not just happen to be correlated, but are subject to the same manipulation, the variation in mechanism sensitivities produced by masking. A few examples of this finding were noted above (see the discussion on CLM's detection contour flanks, for example), but this point is so important it deserves additional emphasis.

Consider as an example the upper flank in Figure 6f. The stimulus at a cone contrast angle of 135°, in the middle of Quadrant II, consists of two cone contrasts that are of equal magnitude but opposite sign, $(\Delta L/L)/(\Delta M/M) = -1$, and a corresponding pair of ratios of modulations of the red, green, and blue primaries of the experimental monitor (r/g, g/b). At threshold in the presence of the 42° noise, this physical/cone modulation is matched with a greenish light on the matching monitor and falls into the green cluster in Figure 6e. However, in the presence of 64° noise, a stimulus consisting of the identical ratio of cone signals (135° in Figure 8f), and the identical pair of experimental monitor primary modulation ratios (r/g, g/b), is matched with a bluish light by the same observer. The appearance changes because the change in noise condition makes G less sensitive than B, according to the detection model, despite each test angle having the same relative cone (or monitor primary) modulations in every noise condition. The threshold color matches are not simply determined by the relative cone modulations, but by which postreceptoral mechanism detects the test.

The basic observation is not new, of course. Similar effects can be found in, for example, the color matching results of Webster and Mollon (1994), who used habituation rather than noise, and in Giulianini and Eskew (1998, dashed line in their figure 3a), who also related the change in appearance to a specific switch of detection mechanisms. Here, however, the correspondence between the detection model (fit only to thresholds) and the color matches, occurs in many cases throughout Figures 5–8 and is very strong evidence supporting the detection model and the univariance and labeled-line assumptions.

Single-cone hues

It has often been reported that, for some subjects and under some conditions, incremental M cone stimuli produce hues that are cyan—more blue than green (e.g., Schirillo & Reeves, 2001). These observations were made with stimuli that were above threshold. The present results show that, at threshold, in cone contrast units the G and B mechanisms have similar sensitivity to $+\Delta M/M$ stimulation, with G more sensitive without noise and with 42° noise, and, for some observers, B somewhat more sensitive with 48° and 64° noises. This sensitivity comparison cannot be made straightforwardly in the (u',v') diagram, due to its arbitrary units and the fact that it is a projective transformation of cone contrast space. The model predicts that suprathreshold M cone increments should stimulate both G and B, with relative sensitivity depending upon conditions.

Similarly, suprathreshold $+\Delta L/L$ stimuli would stimulate the R and O mechanisms, with the balance varying over conditions. Cone decrements also stimulate multiple mechanisms, as shown in all the cone contrast plots; therefore, decremental stimulation of a single cone type could also generate different hues in different conditions.

Mechanism hues

The B and P mechanisms produce blue and purple, hues that are often associated with the S cones, which were not modulated in the present experiment. This is not surprising: standard opponent color theory indicates that a decrement in one cone has an effect that is equivalent to an increment in an opposing cone; here, for example, if the P mechanism gets an S cone input that opposes the L+M input we have measured (Figure 1, Table A1), then the decrements in Quadrant III of cone contrast space would produce the same hue as an increment in the S cones.

The current results indicate a clear and consistent relationship between detection mechanisms and clusters of color matches. One example comes from comparing the overall pattern of matches with the estimated

mechanism directions. As shown in the left panels of Figures 5–8, the chromaticities associated with the quasi-paired mechanisms of Figure 1 do not fall exactly on lines that go through the white point (i.e., they are not colorimetric complements). This is qualitatively consistent with the fact that the cone weights for R and G, for example, are not exactly of equal magnitudes (although they are of opposite sign; see Table A1).

However, quantitatively modeling the relationship between the mechanisms and matches—that is, predicting the actual color matches—is not straightforward. There is a rough correspondence between the clusters of color matches and the segments of mechanism threshold lines shown in the left-hand panels of Figures 5–8. For example, the yellow and purple color match clusters are above and below the white point, and so are the Y and P detection mechanism thresholds. However, there is no unambiguous way to interpret the distance of the clusters from the mechanism lines, because distances and angles in (u′,v′) space have no metric interpretation. Another example comes from comparing differences in angles between the slopes of the mechanism threshold lines and the slope of the line connecting the white point to a color match cluster—the threshold lines are not of constant slope across noise conditions in this projective representation, as noted previously, but the color match clusters do not change position with noise condition.

The color matches are *asymmetric* matches (Wyszecki & Stiles, 1982, chapter 5), since, unlike the tests, the matching stimuli were steadily viewed, suprathreshold, and potentially stimulated the S cones; had they been symmetric matches, they would, in at least many cases, have been matches at the level of the cones, rather than postreceptoral metameric matches, and thus not informative about color appearance. Most importantly, the fact that S cones may contribute to the matching stimuli but not the test stimuli to which they are matched emphasizes the principle that the hues are associated with the postreceptoral mechanisms, not with particular cone types or cone ratios. A threshold response in a single, univariant labeled-line mechanism produces the same hue, regardless of whether that response is based upon signals in the L, M, or S cones.

A remaining question of interest is why the tests near the corners of the detection contour, where the underlying mechanisms have the same sensitivity as one another, do not produce color matches that are mixtures of the matches generated by the two mechanisms when isolated (binary mixtures would produce 11 clusters, counting the number of chromatic angles where two mechanisms have the same sensitivities). For example, a test at 25° that is detected by both the R and Y mechanisms (as seen in Figure 5b) was only matched with a reddish hue (never a yellowish hue) for each of the five matches. Another example is seen in Figure 5f: a test at 64° is close to the corner, and thus perhaps detected by the Y and G mechanisms, but observer SAF only matched this stimulus with a green hue.

In every case for every observer and condition, all five of the matches to a particular test stimulus were located in a single cluster. It is likely that the lack of mixtures is due to a combination of: (a) the test not being exactly in the corner, so that one mechanism response was more salient, and (b) the fact that the matches are memory matches, and likely dominated therefore by the more salient hue. However, it is also possible that there is an actual suppression of one hue—a "winner-take-all" assignment of hue at threshold (A. Stockman, personal communication). The present experiment cannot distinguish these possibilities.

As this discussion indicates, in general, the number of univariant, labeled-line mechanisms is the *minimum* number of color match clusters that should be obtained. Our six-mechanism model could generate anywhere from six to 11 clusters (assuming only binary mixtures), depending on how many of the chosen test angles simultaneously stimulate two mechanisms and how the mixtures that might result are matched in color by the observer. A 12-mechanism model would be expected to generate between 12 and 23 clusters, and a 16-mechanism model between 16 and 31 clusters. Our result is consistent with only a limited number of mechanisms; in principle, six clusters could result from *fewer* than six mechanisms, but not more, and the agreement between the matches and the mechanisms across noise conditions strongly indicates that six is, in fact, the correct number of mechanisms.

General discussion and conclusions

Shepard et al. (2016) presented a chromatic detection model consisting of six linear mechanisms. In that study, we showed that six mechanisms are sufficient to account for selective masking when chromatic noise is placed near the corners of detection contours in the (L,M) plane. Here, in a separate experiment, a color-matching task provided insight into the subjective experience resulting from these mechanisms and also allowed us to test our six-mechanism model. No parameter fitting or model adjustments of any kind were made in order to compare the relationship between the detection model and the color matches. The matches correspond extremely well with the mechanism lines, which allows us to formally apply a color label to each univariant, labeled-line mechanism. Moreover, this correspondence is dynamic: when a change of noise condition changes the pattern of mechanism detection, the color matches change in a corresponding way.

Non-naïve observers

One possible concern with our results is that none of the observers in the experiment were completely naïve, and that their knowledge of the model might have influenced their color matches. Specifically, all of the observers knew that the model predicted six categories of color matches in the entire study. However, in a given noise condition, and thus in a given color matching session, the model actually predicts four, five, or six mechanisms contributing to thresholds (and thus four, five, or six clusters of color matches), with some individual differences. Two of the observers (CLM and SAF) did not know which noise conditions were expected to generate four, five, or six clusters of matches, and they were also not told which noise condition they were being exposed to in any given session (although they could probably guess when the 64° noise was used, since its appearance is quite different from the 42° and 48° noises). Nonetheless, in every noise condition, the number of color match clusters in a particular condition agreed perfectly with the number of mechanisms predicted from that observer's own detection model, whether that was four, five, or six clusters. Most importantly, none of the observers knew which test stimulus was presented at any given time, yet the color matches were almost perfectly consistent with the particular color mechanism that the model asserts detected a given test in a given noise condition.

Putting this all together, the worst-case effect of the observer's knowledge would be that, rather than actually matching the test, they selected a memorized color category that was most similar to the test. We do not believe this happened, but if it did the memorized color would have to be selected on the basis of the test that was seen, since the observers did not know which test was presented. Thus, the most extreme possible effect of their knowledge would be to reduce the variability of the color matches in the clusters, making the task more like color naming than color matching. Even in this case, the pattern of these hypothetical categorical matches would have to consistently change with noise condition in exactly the same way as the detection mechanisms. Our conclusion is that the knowledge of the observers is unlikely to have affected the outcome of this study in a major way.

Discrepancies involving Y and P

In general, the correspondence between the mechanisms of the detection model and the color matches is excellent. However, as mentioned previously, there are three clear discrepancies, all of which involve tests at the ends of the detection contours. In the 42° noise condition for TGS (Figure 6b), the detection model attributes detection of the highest thresholds (those in Quadrant I and those in Quadrant III) to the O and B mechanisms, and the Y and P mechanism lines lie somewhat outside these extreme thresholds. However, the color matches show that both of these sets of thresholds fall into the yellow and purple clusters, not the orange and blue ones. Similarly, a single test (at 64°) in the 64° noise condition for SAF (left-most point in Figure 8e, uppermost point in Figure 8f) should be detected by Y, yet its color match falls in the blue cluster (Figure 8e).

Both of the discrepant cases that involve Y are likely due to the difficulty of accurately estimating the relative cone weights (mechanism angle) of mechanisms at the ends of detection contours, where very few thresholds are available to constrain the mechanism estimates. For TGS (Figure 6b), if the Y threshold line were slightly less steep (i.e., less L cone input), and thus slightly less sensitive to the masking effect of the noise, the result would be that these end thresholds would be detected by Y and would therefore agree with the color matches. For SAF (Figure 8f), increasing the L cone weight to Y (steepening the Y threshold line) would bring the mechanism threshold line nearly into rough agreement with the color match (without significantly altering the overall fit). This alternative Y mechanism threshold is shown in Figure 8f by the dashed line. Compared to the best-fitting Y threshold for SAF (the solid yellow line), the alternative (dashed yellow line) is much more similar to the Y lines of the other two observers (Figure 8b and d). A similar adjustment to the cone weights in P would make the highest thresholds in Quadrant III in Figure 6b (decrement end of the detection contour) detected by P, producing agreement between detection and color matching for those four test angles.

However, it is not likely that simply adjusting the weights of Y and P would alone suffice (as suggested by trial model calculations). The mechanisms in the detection model are all linear (except for rectification), and the model fits are the best estimates of those mechanisms given linear cone combinations (and the constraints of the EvN model). Because the few small discrepancies between detection and hue occur with the highest thresholds, it is quite likely that these mismatches involve nonlinearities in the mechanisms, nonlinearities that were not included in the detection model. Unfortunately, the data do not provide sufficient constraints on the model to estimate such nonlinearities (for discussion, see Shepard et al., 2016).

Alternative models

The color matching experiment helps rule out some alternative models of color mechanisms. As discussed in Shepard et al. (2016), a model containing only four

mechanisms that have adaptive changes in cone weights in the presence of high contrast noises (Atick, Li, & Redlich, 1993; Zaidi & Shapiro, 1993) could fit the entire set of thresholds, simply by altering the cone contrast weights of two of the mechanisms (R and G) in each noise condition to align the long flanks of the detection contour approximately with the noise vector. The other two mechanisms (Y and P) do not necessarily require adaptive weights to account for the pattern of masking. This adaptive model is nearly impossible to test using thresholds alone, without theoretical constraints on the adaptive changes in cone weights. However, the color matching data presented here indicate that the hues of the thresholds fall into six, not four, categories. An adaptive model with only four mechanisms could not easily account for the color matches.

There is no doubt that a model with more than six mechanisms can fit the detection thresholds as well as the six-mechanism model, but as discussed in Shepard et al. (2016), these extra mechanisms do not improve the fit to the thresholds or improve the modeling of selective masking effects. Moreover, quantifying the hues associated with each mechanism, as done here, clearly shows that if there were additional mechanisms, they would have to produce redundant hues. The color matches fall into six categories, not more (or fewer) than six.

None of the threshold stimuli looked achromatic for any of our observers in any of our conditions, and it therefore seems likely that at least one additional pair of mechanisms will eventually be required to account for modulations in three-dimensional cone space in order to create achromatic percepts, making our model have two more mechanisms than the cardinal model. Also, since in these experiments the S cones were not modulated, it is uncertain as to which of the present six mechanisms get S cone input. These are issues still to be settled, and it is of course possible, even likely, that at least one additional pair of mechanisms (an achromatic pair) will ultimately be required. However, the most parsimonious model to account for both detection and threshold-level color matches across a broad range of conditions in the (L,M) plane has six, and only six, mechanisms.

Keywords: color vision, asymmetric color matching, color vision mechanisms

Acknowledgments

This study was supported by NSF Grant BCS-1353338 to RTE. The authors gratefully acknowledge the diligent observing work of Li McCarthy. The manuscript was greatly improved by insightful comments and suggestions made by Andrew Stockman and Greg Horwitz, and we are grateful to A. Logvinenko for first suggesting that we show thresholds in (u′,v′) space.

Commercial relationships: none.
Corresponding author: Timothy G. Shepard.
Email: shepard.197@osu.edu.
Address: College of Optometry, The Ohio State University, Columbus, OH, USA.

Footnote

[1] Although the highly elongated detection contour makes this difficult to see, the purple-colored disk in Quadrant III for CLM (Figure 6d) lies on a color angle that strikes the P mechanism threshold line, not the nearby B line. Therefore, the purple match is correctly predicted by the detection model.

References

Atick, J. J., Li, Z., & Redlich, A. N. (1993). What does post-adaptation color appearance reveal about cortical color representation? *Vision Research*, *33*(1), 123–129, doi:10.1016/0042-6989(93)90065-5.

Brainard, D. H. (1996). Cone contrast and opponent modulation color spaces. In P. K. Kaiser & R. M. Boynton (Eds.), *Human color vision* (2nd ed., pp. 563–579). Washington, DC: Optical Society of America.

Eskew, R. T., Jr. (2008). Chromatic detection and discrimination. In R. H. Masland & T. D. Albright (Eds.), *The senses: A comprehensive reference*. (Vol. 2: Vision II., pp. 101–117). New York: Academic Press.

Eskew, R. T., Jr. (2009). Higher order color mechanisms: A critical review. *Vision Research*, *49*(22), 2686–2704, doi:http://dx.doi.org/10.1016/j.visres.2009.07.005.

Eskew, R. T., Jr., McLellan, J. S., & Giulianini, F. (1999). Chromatic detection and discrimination. In K. R. Gegenfurtner & L. T. Sharpe (Eds.), *Color vision: From genes to perception* (pp. 345–368). Cambridge, UK: Cambridge University Press. doi:10.1016/B978-012370880-9.00302-9.

Estevez, O., & Spekreijse, H. (1982). The "silent substitution" method in visual research. *Vision Research*, *22*(6), 681–691.

Farnsworth, D. (1943). The Farnsworth-Munsell 100-hue and dichotomous tests for color vision. *Journal of the Optical Society of America*, *33*, 568–578, doi:10.1364/JOSA.33.000568.

Giulianini, F., & Eskew, R. T., Jr. (1998). Chromatic masking in the (delta L/L, delta M/M) plane of cone-contrast space reveals only two detection mechanisms. *Vision Research*, *38*(24), 3913–3926, doi:S0042-6989(98)00068-6 [pii].

Giulianini, F., & Eskew, R. T., Jr. (2007). Theory of chromatic noise masking applied to testing linearity of S-cone detection mechanisms. *Journal of the Optical Society of America A: Optics, Image Science, and Vision*, *24*(9), 2604–2621, doi:140122 [pii].

Hansen, T., & Gegenfurtner, K. R. (2006). Higher level chromatic mechanisms for image segmentation. *Journal of Vision*, *6*(3):5, 239–259, doi:10.1167/6.3.5. [PubMed] [Article]

Hansen, T., & Gegenfurtner, K. R. (2013). Higher order color mechanisms: Evidence from noise-masking experiments in cone contrast space. *Journal of Vision*, *13*(1):26, 1–21, doi:10.1167/13.1.26. [PubMed] [Article]

Krauskopf, J. (1999). Higher order color mechanisms. In K. R. Gegenfurtner & L. T. Sharpe (Eds.), *Color vision: From genes to perception*. Cambridge, UK: Cambridge University Press.

Krauskopf, J., Williams, D. R., & Heeley, D. W. (1982). Cardinal directions of color space. *Vision Research*, *22*, 1123–1131, doi:10.1016/0042-6989(82)90077-3.

Krauskopf, J., Williams, D. R., Mandler, M. B., & Brown, A. M. (1986). Higher order color mechanisms. *Vision Research*, *26*(1), 23–32, doi:10.1016/0042-6989(86)90068-4.

Lennie, P., & D'Zmura, M. (1988). Mechanisms of color vision. *Critical Review in Neurobiology*, *3*(4), 333–400.

Li, A., & Lennie, P. (1997). Mechanisms underlying segmentation of colored textures. *Vision Research*, *37*(1), 83–97.

Mullen, K. T., & Kulikowski, J. J. (1990). Wavelength discrimination at detection threshold. *Journal of the Optical Society of America A: Optics, Image Science, and Vision*, *7*(4), 733–742.

Rushton, W. A. H. (1972). Review lecture. Pigments and signals in colour vision. *The Journal of Physiology*, *220*(3), 1P–31P.

Schirillo, J. A., & Reeves, A. (2001). Color-naming of M-cone incremental flashes. *Color Research and Application*, *26*(2), 132–140.

Shepard, T. G., Swanson, E. A., McCarthy, C. L., & Eskew, R. T., Jr. (2016). A model of selective masking in chromatic detection. *Journal of Vision*, *16*(9):3, 1–17, doi:10.1167/16.9.3. [PubMed] [Article]

Wang, Q., Richters, D. P., & Eskew, J. R. T. (2014). Noise masking of S-cone increments and decrements. *Journal of Vision*, *14*(13):8, 1–17, doi:10.1167/14.13.8. [PubMed] [Article]

Watson, A. B., & Robson, J. G. (1981). Discrimination at threshold: Labelled detectors in human vision. *Vision Research*, *21*(7), 1115–1122.

Webster, M. A., & Mollon, J. D. (1994). The influence of contrast adaptation on color appearance. *Vision Research*, *34*(15), 1993–2020.

Wyszecki, G., & Stiles, W. S. (1982). *Color science: Concepts and methods, quantitative data and formulae* (2nd ed.). New York: Wiley.

Zaidi, Q., & Shapiro, A. G. (1993). Adaptive orthogonalization of opponent-color signals. *Biological Cybernetics*, *69*(5–6), 415–428, doi:10.1007/BF01185413.

Appendix

	Log_{10} b	L-cone weight	M-cone weight	Line color
TGS mechanisms				
R	1.35	109.091	−116.985	Red
G	1.39	−111.116	115.064	Green
O	1.10	25.235	−12.857	Orange
B	0.50	−24.979	13.282	Blue
Y	1.57	59.927	19.471	Yellow
P	1.26	−23.468	−37.557	Purple
CLM mechanisms				
R	1.87	315.127	−293.860	Red
G	1.71	−240.235	257.62	Green
O	1.04	96.266	−106.914	Orange
B	1.38	−77.072	66.998	Blue
Y	1.56	55.511	10.790	Yellow
P	1.36	−48.316	−11.155	Purple
SAF mechanisms				
R	1.33	140.075	−166.935	Red
G	2.11	−171.080	183.461	Green
O	6.94	159.973	−77.925	Orange
B	2.19	−123.587	74.259	Blue
Y	1.53	34.044	80.203	Yellow
P	1.28	−28.962	−39.863	Purple

Table A1. Detection model parameters (from Shepard et al., 2016).